

## Full-potential generalized gradient approximation calculations of spiral spin-density waves in $\gamma$ -Fe

D. M. Bylander and Leonard Kleinman

*Department of Physics, University of Texas, Austin, Texas 78712-1081*

(Received 20 October 1998)

Using two different forms of the generalized gradient approximation (GGA) for exchange and correlation, we have performed *ab initio* full-potential calculations of spiral spin-density waves in  $\gamma$ -Fe for wave vectors  $\mathbf{q}=(2\pi/a)(0,0,\alpha)$  and  $\mathbf{q}=(2\pi/a)(\gamma,0,1)$ . We conclude that whereas the local spin-density approximation is merely missing gradient corrections, the GGA contains gradient terms which, although a great improvement in most cases, are inherently incorrect when applied to spiral spin-density waves. [S0163-1829(99)05009-2]

### I. INTRODUCTION

Neutron-scattering experiments<sup>1</sup> on fcc-Fe clusters which have been precipitated out of a Cu matrix demonstrate that their ground state is a spiral spin-density wave (SSDW) with wave vector  $\mathbf{q}=(2\pi/a)(0.1,0,1)$ . Two independent calculations<sup>2,3</sup> using the local spin-density approximation (LSDA) for exchange and correlation (xc) found that  $\mathbf{q}=(2\pi/a)(0,0,0.6)$  was the ground-state wave vector with a local minimum at  $\mathbf{q}=(2\pi/a)(0.5,0,1)$ . When the generalized gradient approximation (GGA) was used, the latter  $\mathbf{q}$  became the ground state.<sup>3</sup> The atomic sphere approximation (ASA) was used in all these calculations. In the ASA, not only is a spherical average of the potential used within the Wigner-Seitz (WS) sphere, but also the magnetization is kept fixed at its average direction within the WS sphere. Because we thought it possible that the discrepancy between theory and experiment could be an artifact of the ASA, we performed<sup>4</sup> a full-potential calculation for  $\gamma$ -Fe in the LSDA, sampling the unit cell at 8000 points and the Brillouin zone at 4000  $\mathbf{k}$  points. Although we found a surprising complexity in the magnetization direction, our energy vs wave vector curve was nearly identical to the ASA curves, having its minimum at  $\mathbf{q}=(2\pi/a)(0,0,0.55)$ . We therefore attributed<sup>4</sup> the discrepancy with experiment to the fact that both the LSDA and GGA are oblivious to the rotation of the magnetization direction, and we then derived an additional term which could be added to the LSDA or GGA to take account of it.<sup>5</sup>

Before applying this correction to the LSDA, we thought it worthwhile to perform full-potential GGA calculations. Although the ASA and full-potential results were nearly identical for the LSDA, there are two reasons they might be different for the GGA. First, the spherical averaging of the charge density in the ASA greatly reduces the magnitude of the gradient, and therefore the differences between the GGA and LSDA results should be much larger in the full-potential calculation. Second, the GGA is essentially a nonlocal approximation, depending on the spin density referred to a fixed quantization axis throughout the entire exchange-correlation hole. Although both the LSDA and GGA can only be applied to the magnitudes of the spin densities referred to a different quantization axis at each point in space,

this does not violate the assumptions behind the LSDA because it is a local approximation, whereas it does violate the aforementioned assumption behind the GGA. Thus it is possible, and the results of this calculation will show, that the addition of a term to the GGA which depends on the rate of rotation of the magnetization will not (at least for the two forms<sup>6,7</sup> of GGA that we use here) result in the correct ground-state wave vector, whereas it likely will when added to the LSDA. Because the ASA takes the magnetization direction to be fixed in each WS sphere, it may be less inconsistent to use an xc approximation which assumes it is fixed in the xc hole than it is in a full-potential calculation. Our method of calculation, using the ultrasoft pseudopotential,<sup>8</sup> is identical to that we used previously<sup>4</sup> with the LSDA except for small changes necessitated by the GGA.

In the next section we obtain equations for the components of the SSDW potential matrix in the GGA and discuss the changes just mentioned. In the last section we present our results and discuss their implication.

### II. GGA FOR SSDW

For noncollinear magnetic systems the GGA exchange-correlation energy functional takes the form

$$E_{xc}[\rho_+, \rho_-] = \int f_{xc}(\rho_+(\mathbf{r}), \rho_-(\mathbf{r}), \nabla\rho_+(\mathbf{r}), \nabla\rho_-(\mathbf{r})) d\mathbf{r}, \quad (1)$$

which differs from the collinear case only in that we have replaced  $\rho_\uparrow$  and  $\rho_\downarrow$  by  $\rho_+$  and  $\rho_-$ . Here,

$$\rho_\pm = \rho/2 \pm m/2, \quad (2)$$

$$\rho = \rho_{\uparrow\uparrow} + \rho_{\downarrow\downarrow}, \quad (3)$$

$$m = \sqrt{(\rho_{\uparrow\uparrow} - \rho_{\downarrow\downarrow})^2 + 4\rho_{\uparrow\downarrow}\rho_{\downarrow\uparrow}}, \quad (4)$$

and the  $\rho_{ij}$  are components of the spin-density matrix. For SSDW's where the magnetization rotates in the  $xy$  plane with no  $z$  component,  $\rho_{\uparrow\uparrow} = \rho_{\downarrow\downarrow}$  and  $\rho_\pm$  simplifies to

$$\rho_\pm = \frac{1}{2}(\rho_{\uparrow\uparrow} + \rho_{\downarrow\downarrow}) \pm (\rho_{\uparrow\downarrow}\rho_{\downarrow\uparrow})^{1/2}. \quad (5)$$

To evaluate the potential,<sup>5</sup>

$$v_{ij} = \delta E_{xc} / \delta \rho_{ji}, \quad (6)$$

we write

$$\begin{aligned} \delta E_{xc} = & \sum_{\sigma=+}^{-} \sum_{i,j} \int \left[ \frac{\partial f_{xc}}{\partial \rho_{\sigma}(\mathbf{r}')} \frac{\partial \rho_{\sigma}(\mathbf{r}')}{\partial \rho_{ij}(\mathbf{r})} \right. \\ & + \frac{\partial f_{xc}}{\partial \nabla \rho_{\sigma}(\mathbf{r}')} \cdot \left( \frac{\partial \nabla \rho_{\sigma}(\mathbf{r}')}{\partial \rho_{ij}(\mathbf{r})} \right. \\ & \left. \left. + \frac{\partial \nabla \rho_{\sigma}(\mathbf{r}')}{\partial \nabla \rho_{ij}(\mathbf{r}')} \frac{\partial \nabla \rho_{ij}(\mathbf{r}')}{\partial \rho_{ij}(\mathbf{r})} \right) \right] d\mathbf{r}' \delta \rho_{ij}(\mathbf{r}) d\mathbf{r}, \quad (7) \end{aligned}$$

and substituting from Eqs. (5) and (6) obtain

$$\begin{aligned} v_{\uparrow\uparrow}(\mathbf{R}) = & v_{\downarrow\downarrow}(\mathbf{R}) \\ = & \frac{1}{2} \sum_{\sigma=+}^{-} \left( \frac{\partial f_{xc}}{\partial \rho_{\sigma}(\mathbf{R})} + \sum_{\mathbf{R}'} \frac{\partial f_{xc}}{\partial \nabla \rho_{\sigma}(\mathbf{R}')} \cdot \frac{\partial \nabla \rho_{\uparrow\uparrow}(\mathbf{R}')}{\partial \rho_{\uparrow\uparrow}(\mathbf{R})} \right), \quad (8) \end{aligned}$$

where we have used  $\partial \rho_{+}(\mathbf{r}) / \partial \rho_{\uparrow\uparrow}(\mathbf{r}') = \partial \rho_{-}(\mathbf{r}) / \partial \rho_{\uparrow\uparrow}(\mathbf{r}') = \frac{1}{2} \delta(\mathbf{r} - \mathbf{r}')$  and, following White and Bird,<sup>9</sup> have replaced the integral in the second term by a sum over points on the fast Fourier transform (FFT) mesh in the unit cell at which the  $\rho_{ij}$  are calculated. Then,

$$\frac{\partial \nabla \rho_{ii}(\mathbf{R}')}{\partial \rho_{ii}(\mathbf{R})} = \frac{1}{N} \sum_{\mathbf{G}} i\mathbf{G} e^{i\mathbf{G} \cdot (\mathbf{R}' - \mathbf{R})} \quad (9)$$

can be used to evaluate  $\partial \nabla \rho_{\uparrow\uparrow}(\mathbf{R}') / \partial \rho_{\uparrow\uparrow}(\mathbf{R})$ . Here  $N$ , the number of reciprocal lattice vectors  $\mathbf{G}$  in which the eigenfunctions are expanded, is equal to the number of real space points  $\mathbf{R}$ .

The determination of  $v_{\uparrow\downarrow} = v_{\downarrow\uparrow}^*$  is only slightly more complicated. From Eqs. (5)–(7) we now obtain

$$\begin{aligned} v_{\uparrow\downarrow}(\mathbf{r}) = & \frac{1}{2} \left[ \frac{\partial f_{xc}}{\partial \rho_{+}(\mathbf{r})} - \frac{\partial f_{xc}}{\partial \rho_{-}(\mathbf{r})} \right] \sqrt{\frac{\rho_{\uparrow\downarrow}(\mathbf{r})}{\rho_{\uparrow\downarrow}(\mathbf{r})}} \\ & + \frac{1}{2} \int \left[ \frac{\partial f_{xc}}{\partial \nabla \rho_{+}(\mathbf{r}')} - \frac{\partial f_{xc}}{\partial \nabla \rho_{-}(\mathbf{r}')} \right] \\ & \times \sqrt{\frac{\rho_{\uparrow\downarrow}(\mathbf{r}')}{\rho_{\uparrow\downarrow}(\mathbf{r}')}} \cdot \left[ \frac{1}{2} \left( \frac{\nabla \rho_{\uparrow\downarrow}(\mathbf{r}')}{\rho_{\uparrow\downarrow}(\mathbf{r}')} - \frac{\nabla \rho_{\uparrow\downarrow}(\mathbf{r}')}{\rho_{\uparrow\downarrow}(\mathbf{r}')} \right) \right. \\ & \left. \times \delta(\mathbf{r} - \mathbf{r}') + \frac{\partial \nabla \rho_{\uparrow\downarrow}(\mathbf{r}')}{\partial \rho_{\uparrow\downarrow}(\mathbf{r})} \right] d\mathbf{r}', \quad (10) \end{aligned}$$

which can be evaluated directly after replacing  $\mathbf{r}$  by  $\mathbf{R}$ , the integral over  $\mathbf{r}'$  by a sum over  $\mathbf{R}'$ , and using

$$\frac{\partial \nabla \rho_{\uparrow\downarrow}(\mathbf{R}')}{\partial \rho_{\uparrow\downarrow}(\mathbf{R})} = -i\mathbf{q} \delta(\mathbf{R}' - \mathbf{R}) + \sum_{\mathbf{G}} i\mathbf{G} e^{i(-\mathbf{q} + \mathbf{G}) \cdot (\mathbf{R}' - \mathbf{R})} \quad (11)$$

for the last term.

Integrating the last term by parts and noting that  $\nabla \sqrt{\rho_{\uparrow\downarrow} / \rho_{\uparrow\downarrow}} = \frac{1}{2} \sqrt{\rho_{\uparrow\downarrow} / \rho_{\uparrow\downarrow}} (\nabla \rho_{\uparrow\downarrow} / \rho_{\uparrow\downarrow} - \nabla \rho_{\uparrow\downarrow} / \rho_{\uparrow\downarrow})$ , this simplifies to

$$\begin{aligned} v_{\uparrow\downarrow}(\mathbf{R}) = & \frac{1}{2} \sqrt{\frac{\rho_{\uparrow\downarrow}(\mathbf{R})}{\rho_{\uparrow\downarrow}(\mathbf{R})}} \left[ \left( \frac{\partial f_{xc}}{\partial \rho_{+}(\mathbf{R})} - \frac{\partial f_{xc}}{\partial \rho_{-}(\mathbf{R})} \right) \right. \\ & \left. - \nabla \cdot \left( \frac{\partial f_{xc}}{\partial \nabla \rho_{+}(\mathbf{R})} - \frac{\partial f_{xc}}{\partial \nabla \rho_{-}(\mathbf{R})} \right) \right]. \quad (12) \end{aligned}$$

Numerical results obtained from Eqs. (10) and (12) differed by hundredths of an meV except for  $\mathbf{q}=0$  and  $(2\pi/a)(0,0,1)$  where they differed by tenths of an meV because  $\rho_{\uparrow\downarrow}(\mathbf{r})$  is real for those  $\mathbf{q}$ 's, allowing it to vanish which causes cusps<sup>11</sup> in  $|\nabla \rho_{\uparrow\downarrow}(\mathbf{r})|$ . Note that because  $\rho_{\uparrow\downarrow} = \rho_{\uparrow\downarrow}^* = |\rho_{\uparrow\downarrow}(\mathbf{R})| e^{i\varphi(\mathbf{R})}$ , where  $\varphi(\mathbf{R})$  is the angle (in the  $xy$  plane) at which the magnetization is pointing,  $\sqrt{\rho_{\uparrow\downarrow}(\mathbf{R})} / \rho_{\uparrow\downarrow}(\mathbf{R}) = e^{i\varphi(\mathbf{R})}$ . If instead of using Eq. (6) we had proceeded as in Ref. 4 to diagonalize the spin-density matrix at every  $\mathbf{R}$  on the FFT mesh, then evaluated the diagonal  $v_{+}(\mathbf{R})$  and  $v_{-}(\mathbf{R})$  matrices, and performed the rotations opposite to those which diagonalized  $\rho_{ij}(\mathbf{R})$ , we would have obtained  $v_{\uparrow\downarrow} = e^{i\varphi(\mathbf{R})} [v_{+}(\mathbf{R}) - v_{-}(\mathbf{R})] / 2$ , which is identical to Eq. (12).

Besides the  $20 \times 20 \times 20$  real and reciprocal space mesh on which most of the calculation is performed, we previously used<sup>4</sup> a  $36 \times 36 \times 36$  real space mesh to evaluate the multipole components of the Coulomb potential which arise from the atomic contributions which must be added to the pseudo-charge density to compensate for the non-norm-conserving nature of the ultrasmooth pseudofunctions<sup>8,10</sup> in addition to evaluating the xc potential arising from the total core plus valence charge density. Here the latter mesh is replaced by a  $45 \times 45 \times 45$  for two reasons. The first is to test the energy dependence on mesh size. The energy change was negligible ( $\sim 0.05$  meV). The second is because for  $\mathbf{q} = (2\pi/a)(0,0,1)$ ,  $\rho_{\uparrow\downarrow}$  is everywhere real and it changes sign on the planes midway between  $[0,0,1]$  atomic planes, causing  $|\nabla \rho_{\uparrow\downarrow}|$  and hence the xc potential to have a cusp on those planes. An odd-numbered mesh avoids those planes.

The scheme we previously used to obtain accurate Fourier transforms of the xc potential is used here in addition to using a similar scheme for evaluating the  $\nabla \rho_{ij}$  which are needed to evaluate the xc potential. We fit  $\rho_{ij}$  as accurately as possible with a spherical function inside an inscribed sphere and subtracted off a smooth function, resulting in a function vanishing at the inscribed sphere. The remaining charge density was fast Fourier transformed, its gradient taken, then fast Fourier transformed back to real space, and added to the gradient of the spherical function.

### III. RESULTS AND CONCLUSIONS

Figure 1 is a plot of the SSDW energy vs wave vector, relative to the energy of the nonmagnetic crystal, calculated with both<sup>6,7</sup> PW91 and Perdew-Burke-Ernzerhot (PBE) xc energy functionals. All calculations are performed at the same lattice constant, 6.822 bohrs, that we used in our LSDA calculations.<sup>4</sup> If we compare our PW91 plot with that obtained<sup>3</sup> using the ASA, we see that the changes from the LSDA plots are similar in direction in that the SSDW states lie higher relative to the ferromagnetic state at  $\Gamma$ , but the changes obtained with the full-potential calculation are much larger. This was perhaps to have been expected because the spherical averaging of the ASA charge density has the effect

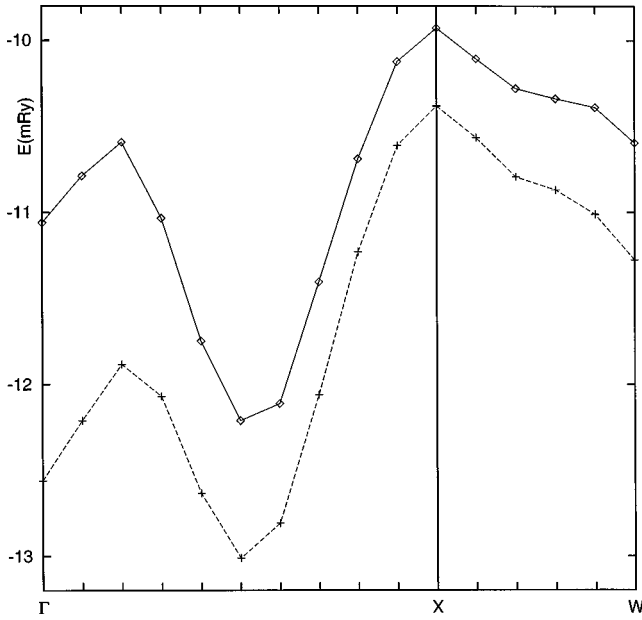


FIG. 1. Energy of the SSDW for wave vectors along the  $\Gamma X$  and  $XW$  lines relative to that of nonmagnetic fcc Fe at the same lattice constant. The dashed (solid) lines represent calculations which used the PBE (PW91) forms of the GGA.

of reducing  $|\nabla\rho_\sigma|$ . The ASA plot for  $a=6.90$  bohrs looks more like the full-potential plot at  $a=6.822$  bohrs than do the ASA plots at  $a=6.80$  or  $6.85$  bohrs, both in that the minimum occurs along  $\Gamma X$  rather than at  $W$  and in that the state at  $X$  lies above that of the ferromagnetic state at  $\Gamma$  only for  $a=6.90$ .

These results indicate that the gradient terms in the GGA are inherently incorrect as opposed to the LSDA, which is merely missing the correct gradient terms. We have recently obtained<sup>5</sup> a term

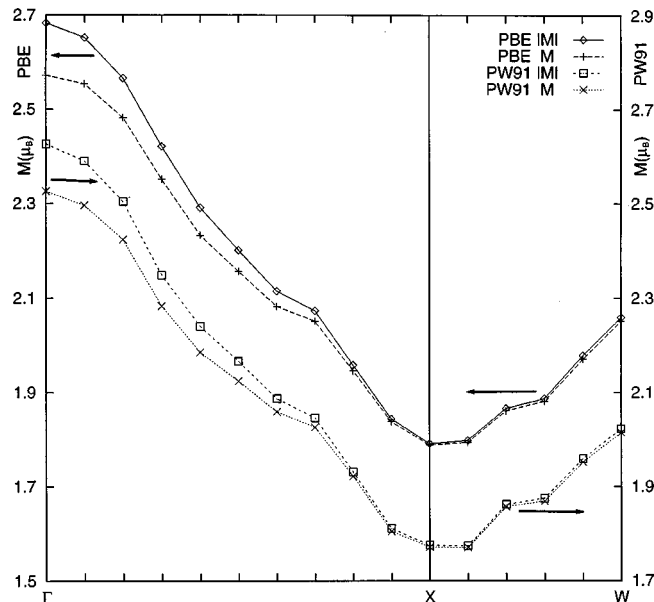


FIG. 2. Integral over the Wigner-Seitz cell of the magnitude of the magnetic moment and of the vector magnetic moment for PBE and PW91 SSDW's with  $\mathbf{q}$  along the  $\Gamma X$  and  $XW$  lines.

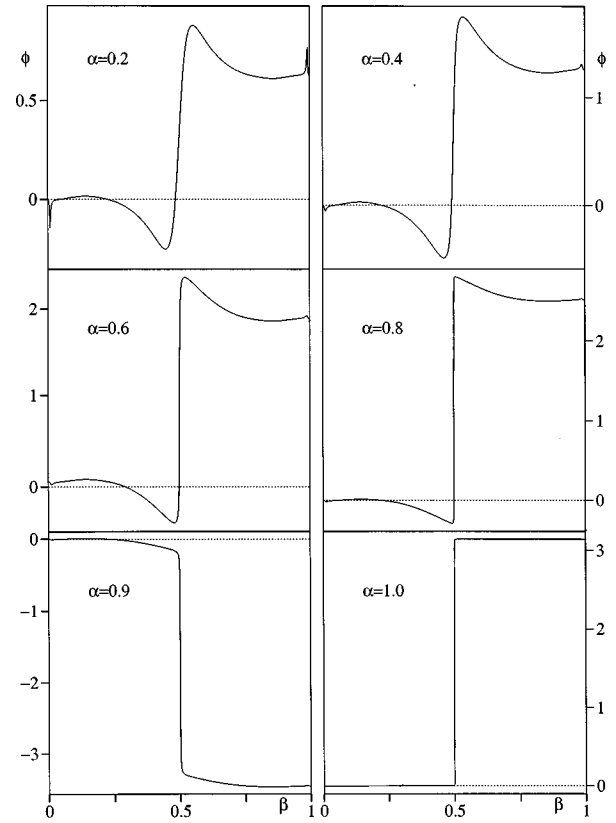


FIG. 3. Phase angle  $\varphi(\mathbf{r})$  of the PW91 SSDW for  $\mathbf{q}=(2\pi/a)(0,0,\alpha)$  and  $\mathbf{r}=\beta(0,\pm a/2,a/2)$  or  $\beta(\pm a/2,0,a/2)$ .

$$\tilde{E}[\{\rho_{ij}\}] = -A \int \frac{(\rho_{\uparrow\downarrow} \nabla \rho_{\uparrow\downarrow} - \rho_{\downarrow\uparrow} \nabla \rho_{\downarrow\uparrow})^2}{\rho^{4/3} \rho_{\uparrow\downarrow} \rho_{\downarrow\uparrow}} d\mathbf{r}, \quad (13)$$

which we suggested (incorrectly as it now turns out) could be added to either the LSDA or GGA density functionals. This term can be rewritten as  $\tilde{E}[\{\rho_{ij}\}] = A \int [|\rho_{\uparrow\downarrow}|^2 (\nabla \varphi)^2 / \rho^{4/3}] d\mathbf{r}$  and thus for a SSDW is proportional to the square of the magnetization times the rate at which its direction is changing.  $A$  is a parameter which the derivation of Eq. (13) suggests should be positive (this makes  $\tilde{E}$  positive because the squared quantity is pure imaginary).  $\tilde{E}$  vanishes at  $\Gamma$  and  $X$  because  $\rho_{\uparrow\downarrow}$  is real for those  $\mathbf{q}$ 's. Thus with the full-potential LSDA where the SSDW at  $X$  was calculated to be 2.695 mRy below the ferromagnetic state at  $\Gamma$ , Eq. (13) with a sufficiently large  $A$  could be used to raise all the other SSDW's above that at  $X$  and, perhaps, with just the right value of  $A$  the energy minimum could be made to occur at  $\mathbf{q}=(2\pi/a)(0.1,0,1)$ , which in the full-potential LSDA was calculated to be 0.275 mRy below  $X$ . With the PW91 GGA (the PBE is worse in this respect)  $\Gamma$  lies 1.16 mRy below  $X$  and 0.98 mRy below the experimental ground state  $\mathbf{q}$ . Thus with the GGA plus Eq. (13) the energy minimum can be made to occur at or near where it does in Fig. 1 or at  $\Gamma$ , but not at or near  $X$ . We are not claiming that the correct GGA consists of the LSDA plus Eq. (13) or even the LSDA plus the exact (to order  $\rho_{\uparrow\downarrow}\rho_{\downarrow\uparrow}$ ) jellium SSDW functional from which Eq. (13) was obtained. The correct GGA for SSDW's must be a functional of  $\nabla\rho_{\uparrow\uparrow}$  and  $\nabla\rho_{\downarrow\downarrow}$  as well as  $\nabla\rho_{\uparrow\downarrow}$  and  $\nabla\rho_{\downarrow\uparrow}$ . What we are saying, however, is that our results in-

dicating that the errors made by ignoring the  $\nabla\rho_{\uparrow\uparrow}$  and  $\nabla\rho_{\downarrow\downarrow}$  contributions do not appear to be fatal, whereas applying a standard GGA to the *magnitude* of the magnetization (i.e., to  $\rho_+$  and  $\rho_-$ ) results in errors which cannot be corrected by adding a functional of the rate at which the direction of the magnetization is changing.

Figure 2 contains plots vs wave vector of the vector magnetization as well as the magnitude of the magnetization integrated over a WS cell. Note that the PBE magnetization is greater than the PW91, which is greater than the LSDA. This ordering is consistent with the ordering of their magnetic energies,<sup>12</sup>  $E_T(\text{nonmag}) - E_T(\text{mag})$ .

In Ref. 4 we incorrectly stated that the vector and scalar magnetization curves became equal at  $X$  because at  $X$  the SSDW becomes antiferromagnetic. However, it is a planar antiferromagnet with the spin polarization changing sign midway between  $[0,0,1]$  atomic planes. The WS cell about an atom of one spin extends all the way to the next atomic plane and therefore has corners containing spin of the opposite sign. In the LSDA calculations this opposite spin was, unlike here, too small to be visible in the plots.

Figure 3 consists of plots of the PW91 SSDW rotation angle  $\varphi(\mathbf{r})$  for  $\mathbf{q}=(2\pi/a)(0,0,\alpha)$  along the nearest-neighbor directions  $\mathbf{r}=\beta(0,\pm a/2,a/2)$  or  $\beta(\pm a/2,0,a/2)$ . The net rotation of the magnetization between neighbors is  $\alpha\pi$  or  $\alpha\pi - 2\pi$ . With the LSDA, whenever  $0.5 \leq \alpha < 1$ , the rotation was  $\alpha\pi - 2\pi$ . Here we only found it for  $\alpha=0.9$ . Otherwise, the plots are similar to the LSDA plots. If one writes  $\rho_{\uparrow\downarrow}(\mathbf{r})=e^{i\mathbf{q}\cdot\mathbf{r}}\tilde{\rho}_{\uparrow\downarrow}(\mathbf{r})$ , one finds that  $\text{Im}\tilde{\rho}_{\uparrow\downarrow}$  is odd, changing

sign midway between neighbors, while  $\text{Re}\tilde{\rho}_{\uparrow\downarrow}$  is even. If  $\text{Re}\tilde{\rho}_{\uparrow\downarrow}$  is positive along the line between neighbors, then  $\Delta\varphi=\alpha\pi$ , but when it changes sign twice,<sup>13</sup>  $\Delta\varphi=\alpha\pi - 2\pi$ . For  $\alpha=0.8$  and  $0.9$ ,  $\tilde{\rho}_{\uparrow\downarrow}$  was so small in the midregion between atoms that it required more than 20 iterations after the energy had converged to pin down its sign. The sign might very well have changed for either of these  $\alpha$ 's had we evaluated  $v_{\uparrow\downarrow}$  using Eq. (12) rather than Eq. (10). Thus whether  $\Delta\varphi$  is  $\alpha\pi$  or  $\alpha\pi - 2\pi$  is really a distinction without a difference, at least when  $\rho_{\uparrow\downarrow}$  is very small midway between the atoms. We see at  $X$  that  $\varphi$  changes discontinuously from 0 to  $\pi$  at the plane midway between atomic planes because, as explained previously<sup>4</sup> for the LSDA,  $\rho_{\uparrow\downarrow}(\mathbf{r})$  is real and changes sign at midplane.

In conclusion, we have performed full-potential calculations of the SSDW energy and magnetization of  $\gamma$ -Fe as a function of wave vector using two different forms of the GGA. Our most important finding was that, unlike the LSDA, the GGA results cannot be made to agree with experiment by the addition of a term depending on the gradient of the angle at which the magnetization is pointing.

#### ACKNOWLEDGMENTS

These calculations were performed at the Texas Advanced Computing Center of the University of Texas at Austin and are supported by the University and NPACI. The research was supported by the Welch Foundation (Houston, TX) and the NSF under Grant No. DMR-9614040.

<sup>1</sup>Y. Tsunoda, Y. Nishioka, and R. M. Nicklow, *J. Magn. Magn. Mater.* **128**, 133 (1993).

<sup>2</sup>M. Uhl, L. M. Sandratskii, and J. Kübler, *J. Magn. Magn. Mater.* **103**, 314 (1992).

<sup>3</sup>M. Körling and J. Ergon, *Phys. Rev. B* **54**, 8293 (1996).

<sup>4</sup>D. M. Bylander and Leonard Kleinman, *Phys. Rev. B* **58**, 9207 (1998).

<sup>5</sup>Leonard Kleinman, *Phys. Rev. B* **59**, 3314 (1999).

<sup>6</sup>J. P. Perdew, in *Electronic Structure of Solids 1991*, edited by P. Ziesche and H. Eschrig (Akademie-Verlag, Berlin, 1991), Vol. 11 (hereafter referred to as PW 91).

<sup>7</sup>J. P. Perdew, K. Burke, and M. Ernzerhof, *Phys. Rev. Lett.* **77**, 3865 (1996).

<sup>8</sup>David Vanderbilt, *Phys. Rev. B* **41**, 7892 (1990).

<sup>9</sup>J. A. White and D. M. Bird, *Phys. Rev. B* **50**, 4954 (1994).

<sup>10</sup>K. Laasonen, A. Pasquardlo, R. Car, C. Lee, and D. Vanderbilt, *Phys. Rev. B* **47**, 10 142 (1993).

<sup>11</sup>Equation (10) does somewhat better than Eq. (12). If we treat  $\mathbf{q}=0$  as a ferromagnet with a  $\rho_{\uparrow}$  and  $\rho_{\downarrow}$  (i.e., no  $\rho_{\uparrow\downarrow}$  and therefore no cusps), we obtain an energy 0.3 meV more negative than that obtained from Eq. (10) and 0.6 meV below that obtained from Eq. (12).

<sup>12</sup>Because of the nonlinear dependence of the xc energy on the charge density, we include the core plus valence xc energy in  $E_T$ , the total valence electron energy.

<sup>13</sup>It is  $\rho_{\uparrow\downarrow}(\mathbf{r})$  that controls  $\Delta\varphi$ ; however, when  $\text{Re}\tilde{\rho}_{\uparrow\downarrow}(\mathbf{r})$  changes sign twice, so does  $\text{Re}\rho_{\uparrow\downarrow}(\mathbf{r})$ .